ISSN 2071-2898 (Print)
ISSN 2071-2901 (Online)

M.L. Battagliere, F. Grazziani, N.V. Kupriyanova, M. Y. Ovchinnikov, V.I. Pen'kov

Design, building and experimental results of a facility to test hysteresis rod parameters

Recommended form of bibliographic references: Battagliere M.L., Grazziani F., Kupriyanova N.V., Ovchinnikov M. Y., Pen'kov V.I. Design, building and experimental results of a facility to test hysteresis rod parameters // Keldysh Institute Preprints. 2007. No. 65. 27 p.
https://library.keldysh.ru/preprint.asp?id=2007-65&lg=e

1. INTRODUCTION

Passive Magnetic Attitude Control System (PMACS) is one of the most common attitude control system implemented on board of small satellites launched in orbit to perform low cost or high risk scientific experiments [1,2]. The aim of a nanosatellite use is to test in orbit new technology and to check ideas under a limited budget and short time for a development [3, 4, 5, 6]. Students of the School of Aerospace Engineering of University “La Sapienza” of Rome and Moscow Institute of Physics and Technology participate in development of PMACS [7, 8].

Choice of attitude control system is based on mission requirements, mission profile, requirements of the scientific instrumentation and requirements of satellite angular motion. In many cases, in actual fact the microsatellite or nanosatellite does not require high precision of orientation or complicated manoeuvres during the flight. Additionally, it can be preferable to avoid movable parts and to limit consume of energy and resources of the satellite and at long last another important requirement can be that the system is as low cost as possible. PMACS satisfies all these requirements [1, 9]. Usually it consists of a strong permanent magnet and energy dissipation system based on magnetic hysteresis rods. Axis of the permanent magnet is aligned with the oriented axis of the satellite in order to provide a restoring torque which aligns the satellite with Earth magnetic field. During motion of the satellite along the orbit the magnetic field direction changes, consequently the satellite oscillates around the direction of the magnetic field. To reduce amplitude of the oscillations a set of hysteresis rods in the equatorial plane of the permanent magnet is used as an energy dissipating system [8, 10]. This system provides also an initial dissipation to reduce oscillations due to ejection from a launcher [8]. The rods are made from magnetically soft material and their parameters depend strongly on manufacturing process and heat treatment; so it is not so easy to predict theoretically their behaviour. Rods efficiency depends on their volume, material used, technique of heat treatment, elongation (i.e. ratio of the length of rod to its diameter) and also on their arrangement on board of the satellite. In fact, it is well known that hysteresis rods influence mutually each other (demagnetization effect) [11] and that the best arrangement of hysteresis rods in the satellite body is to place these rods far from permanent magnet as much as possible; but these requirements are not satisfied when size of satellite is too small as in the case of a nanosatellite. In other hand, for the previous ten years a great increase of nanosatellite production tool place, mostly at universities and with “Cubesat” program coming after 2000 [12].

Ten years ago about 14 university spacecrafts had been launched [13]. Nowadays about 62 university-built spacecrafts have already been launched (and, at least, other 25 are scheduled to be launched in 2006/2007) by about 50 university teams in various countries of the world [14]. This trend in the space research and university teaching activity, as well as the necessity to develop an accurate modelling of the hysteresis rods magnetization to predict performance in orbit of PMACS suggested idea to develop a simple facility to perform tests in laboratory of the hysteresis rods[1] [15]. Main goal of these experimental activity carried out at the Keldysh Institute of Applied Mathematics of Russian Academy of Science (KIAM RAS) is to analyze the behaviour of hysteresis rods of two different kinds in presence of external magnetic field along the rod and to compare these results with the results obtained using the model already developed at KIAM RAS and incorporated to the developing of the PMACS of TNS-0 nanosatellite [15]. In this issue the design, realization and test of the facility is described and preliminary results of the tests carried out on the hysteresis rods are shown.

2. DESIGN AND REALIZATION OF A FACILTY TO CARRY OUT TEST OF THE HYSTERESIS RODS MAGNETIZATION

The facility to test hysteresis rods magnetization is based on a simple circuit. There is a transformer which provides the power supply. The transformer is connected with a variable resistor in parallel with a solenoid. The transformer has been modified to provide a variable voltage of about 19 V (V_p) in input of $f = 50$ Hz frequency. Variable resistor provides a maximum resistance of about 7.6 kOhm and it is utilized in the scheme to change the value of the current which flows in the circuit. In this way it is possible to test behaviour of hysteresis rods at changing of magnetic field applied. After that, there is a solenoid realized with a copper wire rolled up at plastic cylindrical body with a diameter of 0.75 cm. Resistor and main coil have been arranged on a wood base. Main parameters of the facility are resumed in the Table 1 and shown in Fig.1. Facility under realization and final arrangement are visible in Fig.2. In the Table 1 the resistance of the coil-1 has been calculated on the basis of well known formulas [16] and measured with a tester

$$R_1 = \rho \frac{l_{w-1}}{S_w}. \tag{2.1}$$

All symbols in this expression have already been explained in the list of symbols at the Appendix 3. To size coil-1 the following formulas [16] have been used

$$H = \frac{N_1 i}{L_1}, \tag{2.2}$$

where H, the Earth magnetic field intensity and L_1, the length of coil-1 are known; in this way there are two independent parameters, N_1 and $, i$ and the current can been modified using the variable resistor.

[1] Idea to develop and build a laboratory facility for hyteresis rod parameters exploration in combination with advanced numerical model was suggested by Dr.Vladimir Pen’kov.

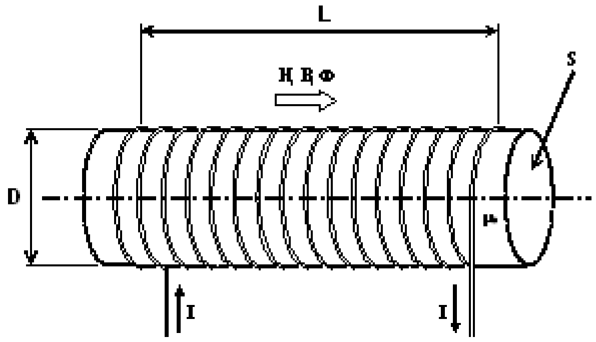

Fig.1. Main parameters of coil

Table 1. Main parameters of coil-1 and of the facility to test hysteresis rods magnetization

Transformer	220 V to 19 V (alternative), 50 Hz
Resistor (R_p)	0 - 7.5 kOhm
Measured Resistance of coil-1	134 Ohm
Resistivity of wire	$1.7 \cdot 10^{-8}$ Ohm · m
D_1	7.5 mm
Section of wire	$7 \cdot 10^{-9}$ m^2
N_1	2342
Length of wire for coil-1	$2\pi \frac{D_1}{2} N_1 = 58.9$ m
L_1	25 cm
H inside of the solenoid	1361 A/m (max)
B inside of the solenoid	$1.7 \cdot 10^{-3}$ T (max)
Inductance of coil-1	1.27 mH


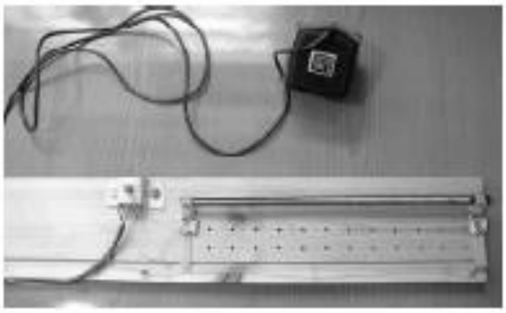

Fig.2. Facility during the realization (left) and final assembling (right)

Number of loops for coil-1 has been chosen considering also that solenoid had to cover whole length of hysteresis rod to evaluate rod parameters changing position of the second coil. As a reference we considered for H_E values variable from 0.31 and 0.62 Oe (24.68 A/m and 49.36 A/m) on the Earth surface; value of Earth magnetic field in LEO (Low Earth Orbit), for example at 500 km of height, is 19.68 A/m over the equator and 39.60 A/m over the poles. Maximum value of magnetic field inside of the solenoid (B) is approximately $1.7 \cdot 10^{-3}$ T. It corresponds to $H = 1361$ A/m. In this case hysteresis rod is saturated. We can estimate the intensity of saturation for the available rods for testing is approximately 50 A/m. Using variable resistor the value of current which flows in the solenoid and then the value of B inside of coil-1 are changed.

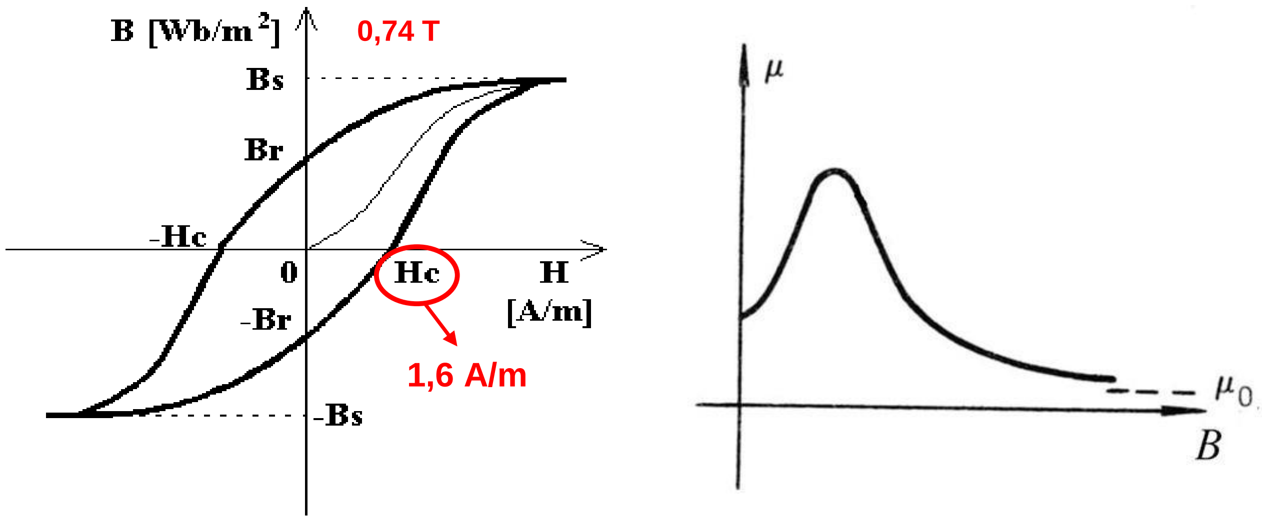

Fig.3. An example of hysteresis loop for a ferromagnetic material (left). In the diagram the values of saturation and coercitive fields for hysteresis rod-1 available for test in laboratory are shown. The trend of magnetic permeability of a ferromagnetic material when B changes is presented (right)

A typical hysteresis loop which shows the relation between magnetizing field and induction for a ferromagnetic material is available (Fig.3). Main notations are: B_s is a saturation induction, B_r is a residual induction, H_c is a coercitive force. Shape of this cycle depends on an amplitude of H_c, material, its remagnetization history. Area inside of the cycle is proportional to dissipated energy during a cycle [16]. In the right the trend of magnetic permeability depending of B is shown. The permeability begins by an initial value which corresponds at inclination of curve of first magnetization in the origin and grows until maximum value. After that it decreases and inclines to the value of an initial permeability [16]. After such a brief summary of main parameters of the ferromagnetic material and non-linearity of the magnetic permeability an idea of this experimental activity is discussed.

Working principle of this facility is based on induction law of Newman-Faraday-Lenz, that is, while a variable current flows in the coil-1 it generates in a secondary coil an induced electromagnetic force. The secondary coil (coil-2) is used as a sensor which moves along the solenoid (coil-1). We see signals from coils on oscilloscope screen. Channel-1 of oscilloscope is connected to the coil-1, channel-2 is connected to the coil-2. During the first step of the work the idea is to observe Lissajous's pictures (Appendix 1) generated by these two signals and to establish the relation between inclination of Lissajous's ellipse which depends on difference of phase of two signals and rod permeability along its length. Nevertheless, the non-linearity of the ferromagnetic material (Fig.3) which composes the rod limits the possibility to see a regular ellipse of Lissajous.

At the end of this section the problem of sizing of secondary coil and choice of its placing with respect to the coil-1 is considered.

Magnetic field inside of coil-1 is calculated using the formulas [16]

$$B = \mu_0 \frac{N_1}{L_1} i \qquad (2.3)$$

where the magnetic permeability of vacuum μ_0 is equal to $12.56 \cdot 10^{-7}$ $(\mathrm{Wb} \cdot \mathrm{m}^2)/\mathrm{A}$. Formulas (2.3) is valid for a solenoid with $L >> r$ (length of solenoid is much more than radius of solenoid cross section) and not near extremities of solenoid. Induced flux in the secondary coil is expressed by [16]

$$\Phi_2 = B_1 N_2 S_2, \qquad (2.4)$$

where B_1 is the magnetic field induction inside of the coil-1, N_2 is a number of loops of coil-2 and S_2 is the cross section of coil-2. Induced electromagnetic force in the coil-2 is evaluated on the basis of the following set of formula [16]

$$E_{ind} = -\frac{d\Phi_2}{dt} = -\mu_0 \frac{N_1 N_2}{L_1} S_2 \frac{dI(t)}{dt}. \qquad (2.5)$$

Presence of factor μ_0 reduces remarkably the amplitude of signal of the coil-2 (≈mV). It means that it is important to evaluate N_2 in way in order to get a visible signal on the screen of the oscilloscope considering also the presence of electromagnetic noise due to electrical network at 50 Hz within the laboratory. To watch a signal on the channel-2 we fixed its amplitude $A_2 >> A_{noise}$, that is, $A_2 >> 6-8$ mV and $A_2 \approx 20-30$ mV at least. On the basis of this requirement the number of loops of coil-2 has been fixed at about 1500, so that $A_2 \approx 45$ mV. Test demonstrated that hysteresis rod amplifies this signal in about 20 times. Main parameters of coil-2 are sketched in the Table 2.

Table 2. Main parameters of coil-2 of the facility for testing of hysteresis rods magnetization

Measured resistance of coil-2, R_2	178 Ohm
Resistivity of wire	$1.7\cdot10^{-8}$ Ohm$\cdot$m
D_2	1.5 cm
Cross section S_2	$1.77\cdot10^{-4}$ m^2
N_2	1550
Length of wire for coil-2	$2\pi\frac{D_2}{2}N_2 = 73$ m
L_2	2 cm
Section of wire	$7\cdot10^{-9}$ m^2
Inductance of coil-2	26.7 mH

The next step has been to establish the better way to arrange the secondary coil with respect to the first coil to carry out measurements. Signal of the coil-2 depends also on position of coil-2 with respect to the field generated by coil-1. Signal is maximum when plane of the coils is perpendicular to force lines of field generated by coil-1 and minimum while the plan is parallel to the force lines. To maximize the factor of the mutual induction the scheme of arrangement sketched in Fig.4 has been chosen.

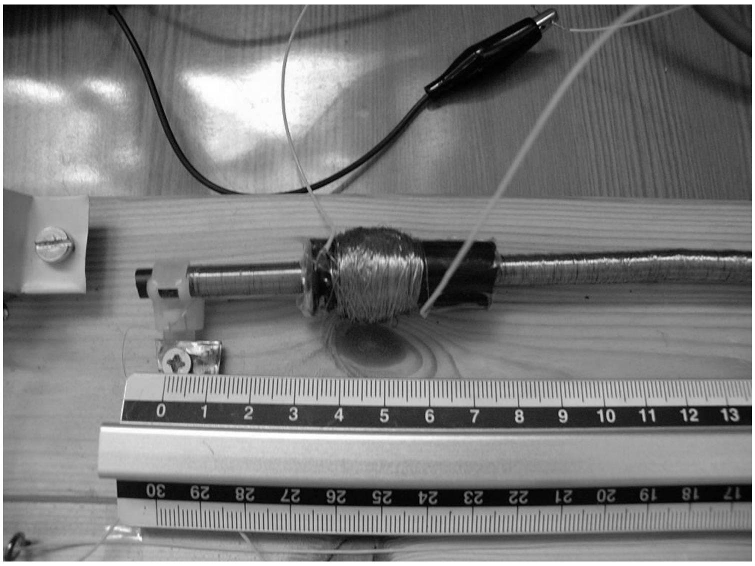

Fig.4. Scheme of arrangement of the coil-2 with respect to the coil-1

To move coil-2 along the coil-1 in a very simple way we measure punctual properties of the hysteresis rods placed inside of cylindrical support of coil-1.

3. FIRST TEST OF THE FACILITY: EXISTENCE OF THE EARTH MAGNETIC FIELD AND EFFECT OF HYSTERESIS RODS ON THE MAGNETIC FIELD INSIDE OF THE SOLENOID

A first elementary test has been performed to check functioning of the facility. This test allowed us, also, to confirm variation of the rod parameters along its length. A compass has been placed near the coil-1 without to supply the facility and without a rod inside the core of solenoid. Magnetic needle of compass finds one's bearings in the magnetic north direction (approximately 11.5 degrees far from geographic north direction). In this test we are not interested in the quantitative results but qualitative analysis in only. For this test it has been necessary to put a diode to supply facility with a continue current because we need of a constant field which changes direction of the compass needle. In this way we verify that facility works generating a magnetic field inside of the solenoid. To do this a check alimentation has been switched on. During this experience the value of variable resistor was fixed at 10 kOhm which corresponds to $B = 2.38 \cdot 10^{-5}$ T. This value was comparable with value of Earth magnetic field which lies on the Earth surface approximately in the range from $3.1 \cdot 10^{-5}$ T to $6.2 \cdot 10^{-5}$ T. The compass needle did not change in a remarkable way but to verify the correct working of facility it was enough to put one hysteresis rod inside of core of solenoid: suddenly compass needle changed its position moving of about 15 degrees. In the pictures 1 and 3 of Fig.5 one sees this angular motion of the compass needle.

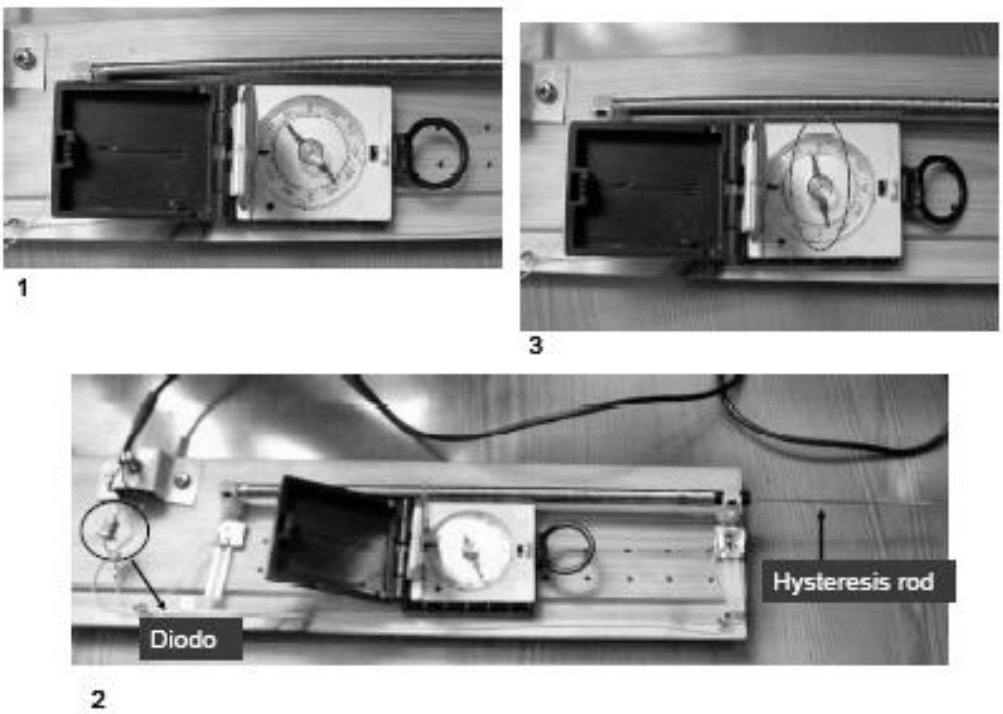

Fig.5. First test of working of the facility

Moving hysteresis rod inside of coil-1 great variations of the angle have been measured. This result confirmed the interest in the goal of this work, that is, to try to explain in which way parameters of the hysteresis rod change along its length and to develop a modelling useful for next applications on board of small satellites.

4. SECOND TEST OF THE FACILITY: A RLC CIRCUIT TO VERIFY LISSAJOUS FIGURES AT THE OSCILLOSCOPE SCREEN

A second test has been performed to check the instrumentation available in the laboratory with aim to avoid uncertainties in the analysis of the results of tests on the hysteresis rods during the next experimental activity. The test has been carried out using a RLC circuit (Fig.6) with the main goal to check Lissajous's pictures visible on the screen of the oscilloscope depending of different kind of signals in input. The part RC of circuit has been sized (Appendix 2) in way to have two signals with the same amplitude to obtain a Lissajous's circle. Three resistances has been soldered in series in order to obtain a total resistance of about 1.4 kOhm. Capacitor has been chosen to obtain a signal with the same amplitude (V_C) of the resistance (V_R). Its capacity is equal to 2.28 μF. As inductance has been chosen during the tests it has been possible to establish that the coil-1 behaved as a resistance because its inductance is very small. In fact a calculation of this inductance demonstrated that its value is approximately equal to 1.2 mH, whereas its measured resistance is 134 Ohm. In any case this fact did not restrict results of the test because the idea was to use signals with different phases to confirm theoretically expected Lissajous's pictures and it was done with a RC circuit.

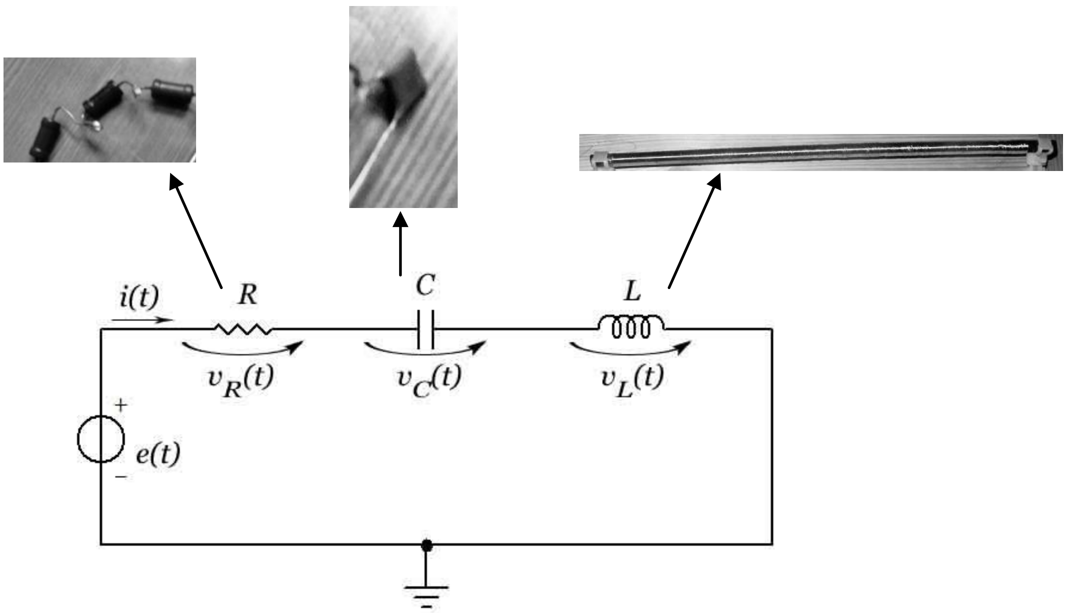

Fig.6. Circuit RLC used to test operative way X-Y in the oscilloscope

Results obtained by connecting channel-1 of the oscilloscope with resistance and channel-2 with capacitor are shown in Fig.7. Amplitude of signal is about the same ($R = 1.345$ kOhm and capacitive reactance $X_C = -\frac{1}{\omega C} = 1.4$ kOhm) and they have a difference of phases of 90°.

Voltages V_R and V_C measured with oscilloscope correspond at theoretical values. Corresponding Lissajous's picture is an ellipse very close to a circle with small disturbances.

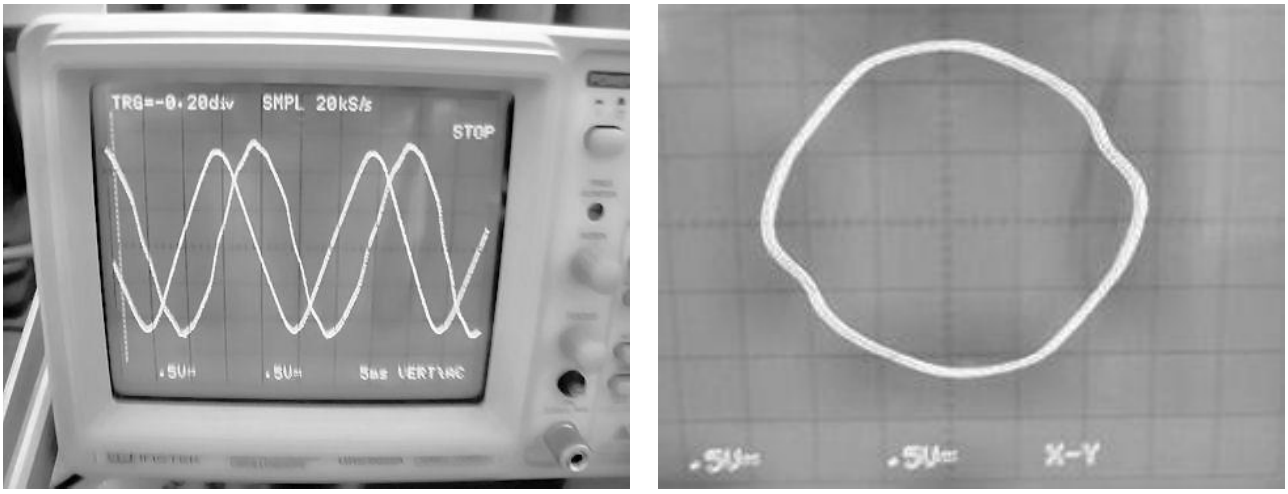

Fig.7. Results for RC circuit: signals with respect to line (left) and corresponding Lissajous's picture (right)

The same test has been carried out by connecting channel-1 and channel-2 of the oscilloscope with the same resistance. In this case Lissajous's picture expected is a line with an inclination of 45°. Results are visible in Fig.8.

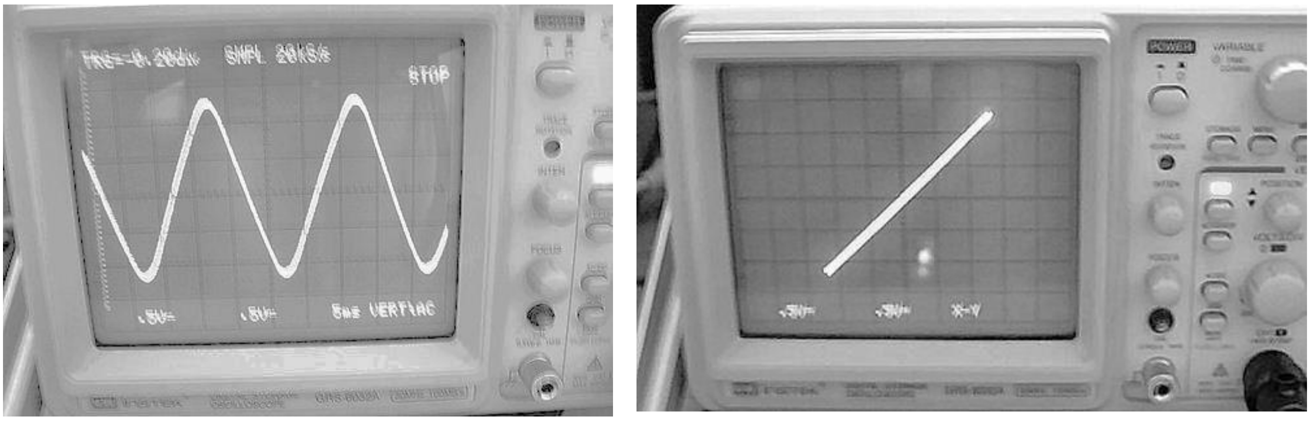

Fig.8. Channel-1 and channel-2 connected at the same signal in input

After, channel-1 has been connected with capacitor and channel-2 with coil-1. Theoretically we exepect a difference of phases $\Delta\varphi = 180°$ and Lissajous's picture is a line with an inclination of 135° but here this coil behaves as a resistance because $X_L << R_1$. Results obtained with measurements confirm it (Fig.9).

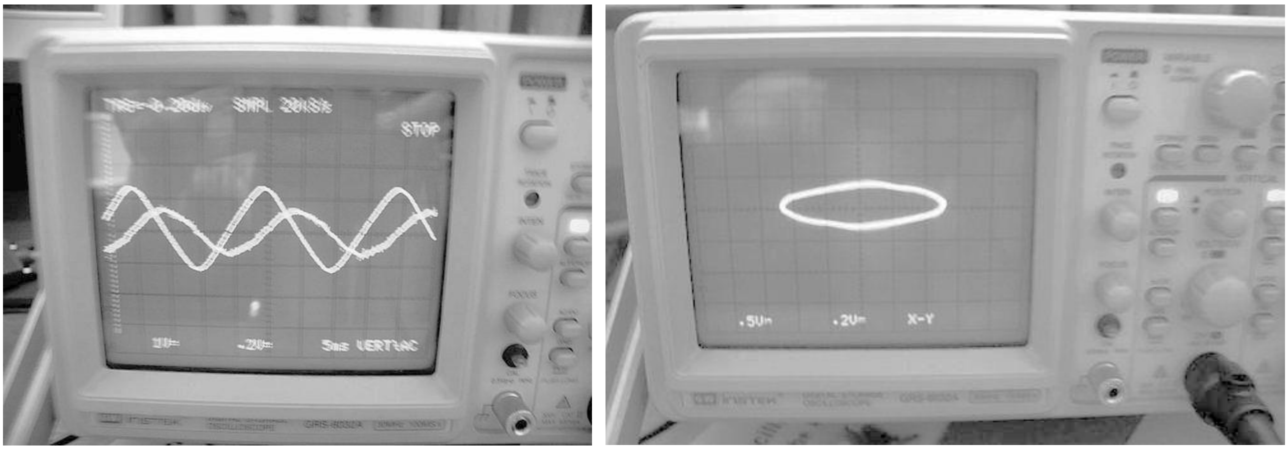

Fig.9. Channel-1 connected at capacitor and channel-2 connected at coil-1

In Fig.8 we see two signals with $\Delta\varphi = 90°$ where the second signal has an amplitude quite less then one of the first signal ($V_C = 12$ V and $V_1 = 2$ V). Correspondent Lissajous's picture is an ellipse without inclination with respect to axis X and Y. At the end, a test has been carried out with a small inductance (10 mH) and a resistance ($R = 150$ Ohm). Result confirmed a difference of phase of 90°. These simple tests allowed us to confirm a correct working of the oscilloscope (after a compensation of the probes) and will be useful in the analysis of signal related with hysteresis rods.

5. THIRD TEST ON THE FACILITY: RESULTS OF TESTS WITHOUT RODS

It is well known [16] that in the extremities of a solenoid when a current flows there is an edge effect which halves the value of internal field. Neglecting values of field in the extremities of the solenoid ($L_1 = 25$ cm), measurements have been carried out from 4 cm of the length of the solenoid to 22 cm to verify the uniformity of inducting field in the central part of the coil-1. Voltage applied at the solenoid is 10 V corresponding to a current $i_0 = 74.63$ mA and to a field $H = 746.3$ A/m inside of the coil-1. Results available in Fig.10 show that there is not a very uniform behaviour of internal field along the coil-1. Probably these results depend on non-uniform distribution of coils during manufacturing process both coil-1 and coil-2. In any case these results have to be taken into account in the analysis of the measurements related to the hysteresis rods.

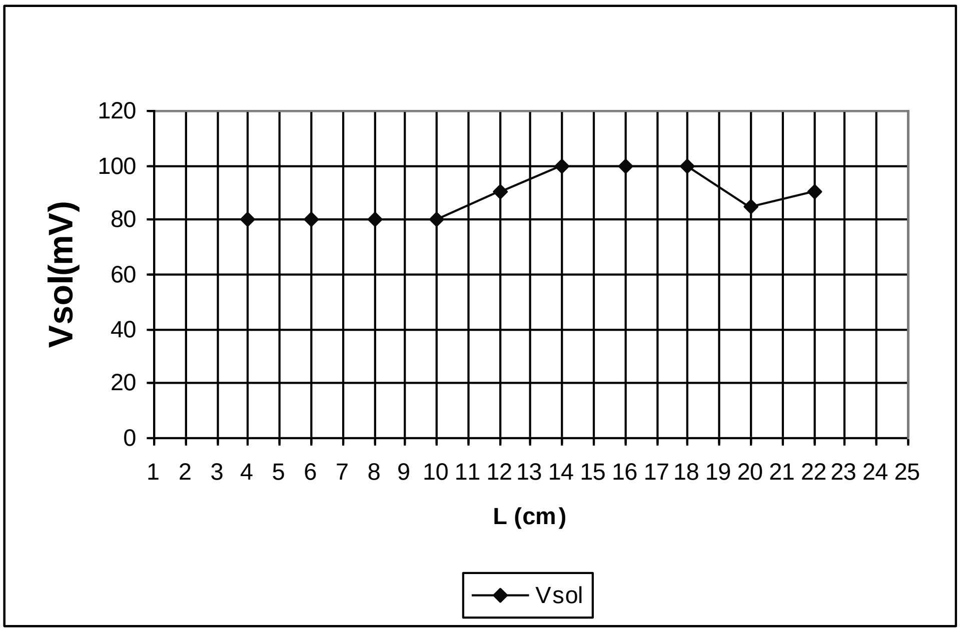

Fig.10. Voltage values measured with coil-2 along the solenoid without rod inside

6. RESULTS OF TESTS CARRIED OUT ON THE HYSTERESIS RODS

Tests have been performed on two different hysteresis rods. The first rod named rod-1 has a length of 25 cm and a section of $1\,\mathrm{mm}\times 1\,\mathrm{mm}$ with a rectangular shape. This type of rod has been utilized on board of MUNIN nanosatellite [10] of Institute of Space Physics of Kiruna (Sweden) launched on 21th of November, 2000 from Vandenberg Air Force Base located on the Central Coast of California with the Delta 7000 Launch Vehicle. Rod-1 has been manufactured with molybdenum permalloy of the 79NM specification; its composition includes 79% of Ni, 4% of Mo and 17% of Fe [10]. Main parameters of the rod are available in Table 3.

Table 3. Main parameters of the rod

Initial magnetic permeability μ_{r_in}	Maximum magnetic permeability $\mu_{r\_\max}$	Coercitive force H_c, [A/m]	Residual induction B_s, [T]	Elongation of rod-1 $p = l/d$
25000	180000	1.6	0.74	250

Second hysteresis rod named rod-2 has a length of 13 cm a section of $2\,\mathrm{mm}\times 2\,\mathrm{mm}$ with a rectangular shape and elongation of p=65. For the rod main parameters are not available but parameters of the material are available in [10, 17].

Information about elongation allows us to do some considerations, that is, the parameter p for rod-2 is very far with respect to the usual optimal values of elongation which lie in the range 200-300 [10]. In our work for reasons of briefness and to give a complete view of the results obtained with experimental tests of the rod-1 it will be refereed only diagrams and results for this rod. Results of rod-2 confirm the same behaviour of the rod-1. The shape of the signal is similar but much more irregularities appear and values of amplitude are greater. Tests have been performed on the hysteresis rod-1 changing the value of the current inside the coil-1. A summary of some values is available in Table 4 where V_{coil} is the voltage applied at coil-1, I_c is a current which flows through the solenoid, H and B are, respectively, the magnetic field intensity and magnetic induction flux inside of the coil-1. In the first case ($V_{coil} = 0.5\ \mathrm{V}$) rod is not in saturation. In the second one the rod approaches the saturation. In the third case rod is in saturation. In the last case we evaluated behaviour of the rod in a limit condition when $H >> H_s$ (H_s is saturation field intensity).

Table 4. Main values of different configurations for test on the hysteresis rod-1

V_{coil} (V)	I_c (mA)	H_{coil} (A/m)	B_{coil} (T)
0.5	3.73	37.30	$4.7 \cdot 10^{-5}$
1.0	7.46	74.63	$9.3 \cdot 10^{-5}$
2.0	14.90	149.25	$18.7 \cdot 10^{-5}$
18.3	136.6	1366	$1.7 \cdot 10^{-3}$

For voltage values $V_{coil} = 0.5\ \mathrm{V}$, $V_{coil} = 1\ \mathrm{V}$ and $V_{coil} = 2\ \mathrm{V}$ it has been verified that signal shape generated by coil-2 in the oscilloscope without rod inside of the solenoid follows cosine law as it is evaluated in the relation (2.5) assuming $i = i_0 \sin \omega t$. The shape of signal related at the rod-1 when $V_{coil} = 0.5\ \mathrm{V}$ and $I_c = 3.73\ \mathrm{mA}$ is sketched in Fig.11. Preliminary results of measuring showed that the magnetic field is maximum in the centre of the rods and minimum at the extremity and it should be noted that there is no important changing in the shape (only in the amplitude) of the signal when the position of the coil-2 varies along the rod-1. Tests have been repeated with the facility arranged in a metallic box to verify if noise occurs in these measurements but results obtained are the same.

To confirm this result about magnetization of the rod tests have been repeated with a different configuration (Fig.11). The goal was to check either the field in the extremities of rod is in different times less with respect to the value in the centre of rod due to the characteristics of magnetization along the rod or this is an effect of the field in extremities of the solenoid and an effect related to results showed in Fig.9.

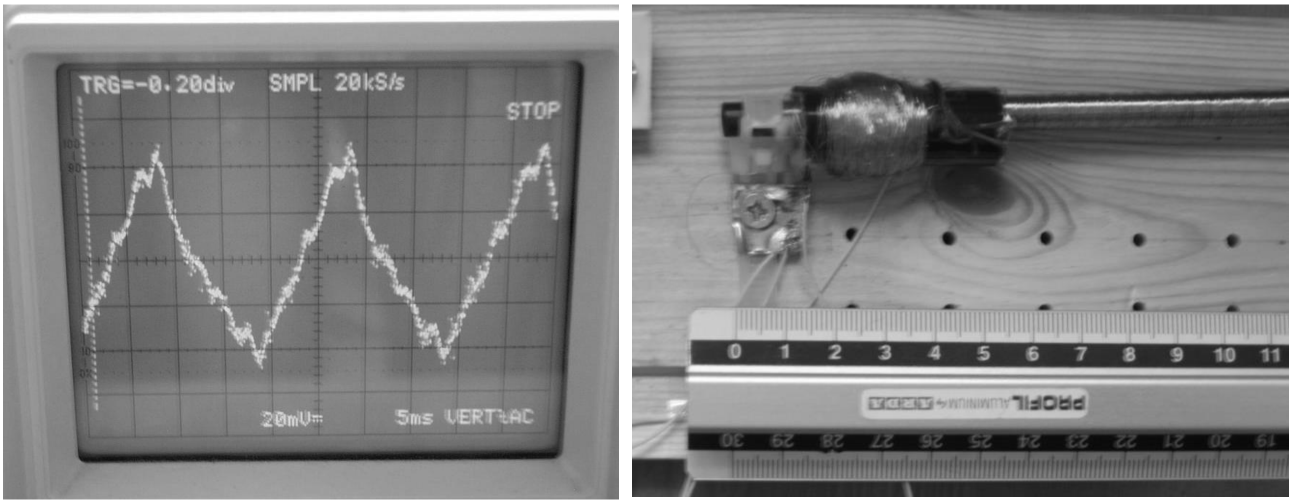

Fig.11. Results of test on the hysteresis rod-1: amplitude of signal is minimum at the extremities and maximum in the centre of rod

In this configuration the coil-2 has been placed in different positions along the solenoid and the rod has been inserted in way to do measurements at its extremity. Scheme of this test with coil-2 arranged in the middle of solenoid (at 10 cm) is shown in Fig.12. Results demonstrated that this trend can be related to the characteristic of the magnetization of the rod.

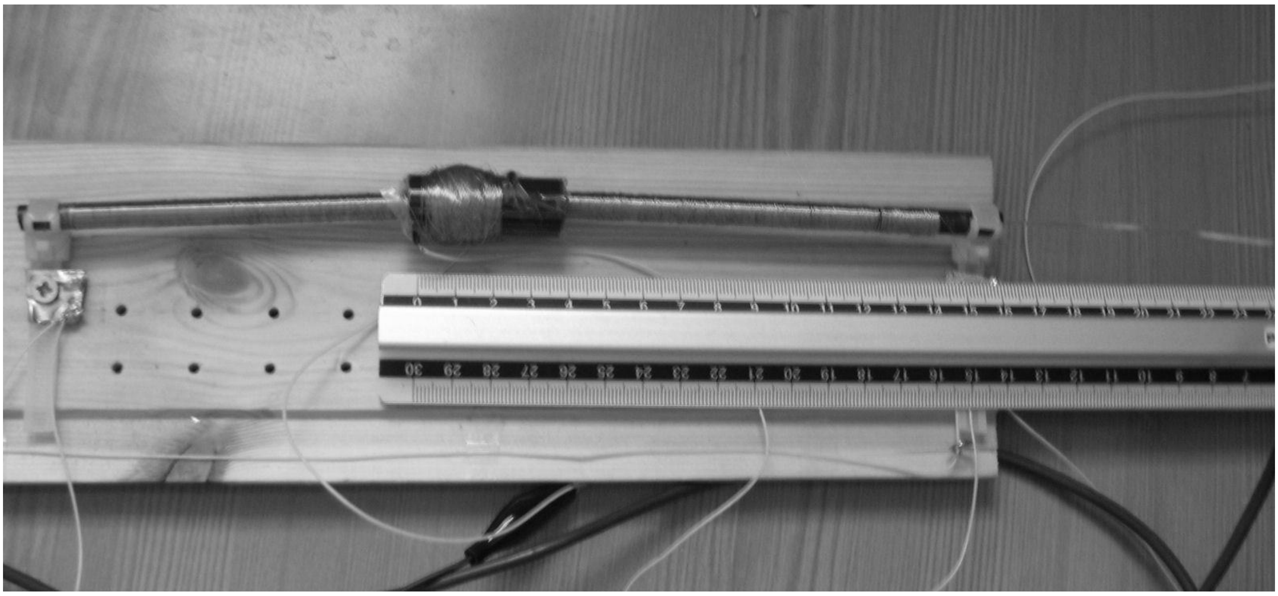

Fig.12. Results of test on the hysteresis rod-1: coil-2 has been placed at 10 cm along the solenoid with respect to the left extremity and hysteresis rod has been inserted in the coil-1 in a way to have the left extremity inside of coil-2

Measurements have been completed by changing inclination of coil-1 with respect to Earth magnetic field whose direction has been specified with the compass. Measurements have been obtained for a random inclination (Series-I: random B_E), in the perpendicular direction of coil-1 with respect to Earth magnetic field direction (Series-II: normal B_E) and in the same direction of Earth magnetic field (Series-III:

parallel B_E). In Fig.13, the diagram of the results obtained with different set of measurements in laboratory is sketched.

These results show that there is no a visible effect of the relative position with respect to the Earth magnetic field direction. Small differences in the measurements can depend on casual errors due to, for example, small differences in the position of coil-2 along coil-1 or in the readings of oscilloscope. When voltage applied to coil-1 increases the shape of signal changes. This changing is visible in Fig.14. Results for hysteresis rod-1 when $V_{coil} = 1$ V and $V_{coil} = 18.3$ V are available in Fig.15 and Fig.16 respectively.

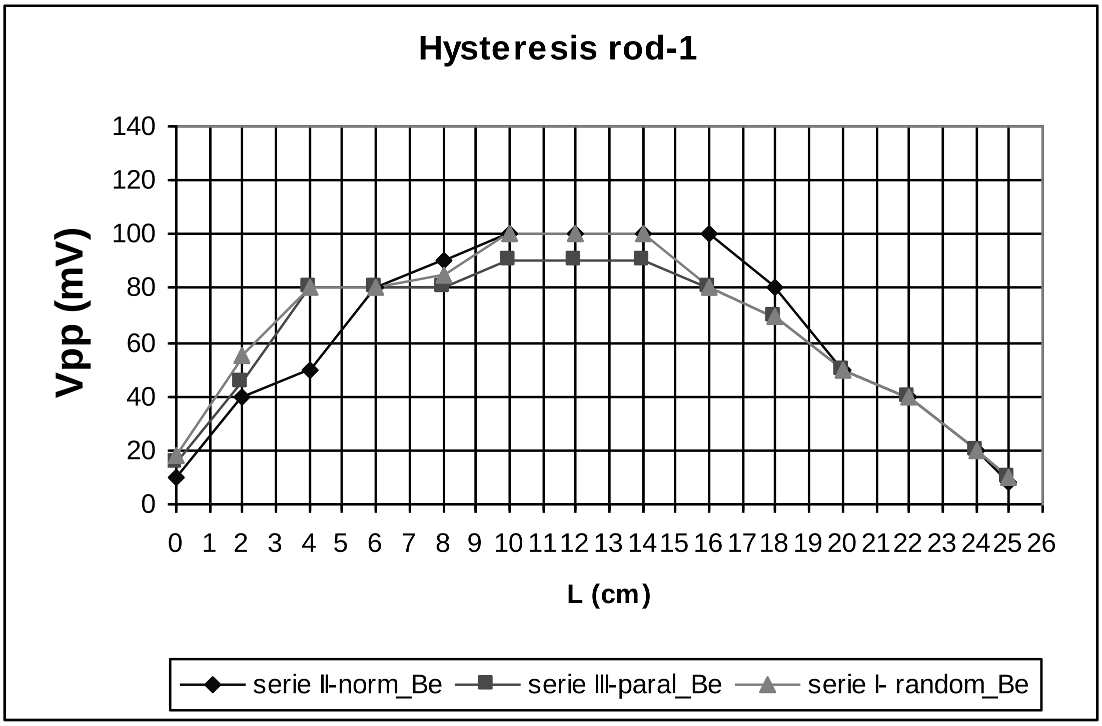

Fig.13. Trend of magnetic field inside of rod-1: X axis represents the length of hysteresis rod, Y axis represents experimentally values obtained during tests in laboratory along the rod-1 for induced voltage in coil-2. Diagram shows 3 set of measurements with different positions of the facility with respect to Earth magnetic field direction

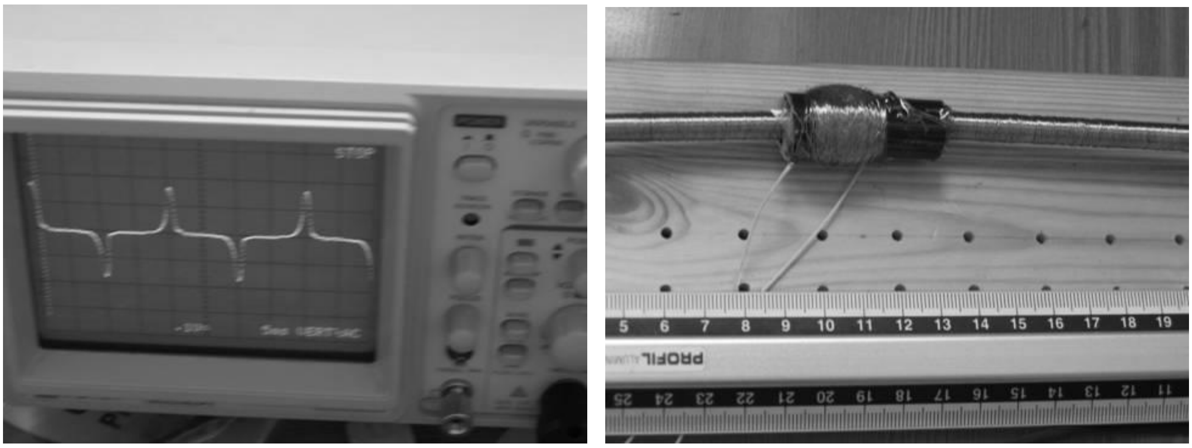

Fig.14. Results of test on the hysteresis rod-1: amplitude of signal is maximum in the centre of rod; in this picture we see signal corresponding at coil-2 placed at about 10.5 cm with respect to the extremity of left of the rod when $V_{coil} = 18.3$ V

Results for $V_{coil} = 2$ V confirm the same behaviour of these two previous cases. At this step of work we can not establish if this changing depends by saturation of the rod or not. There are not visible effects of the relative position between rod and Earth magnetic field.

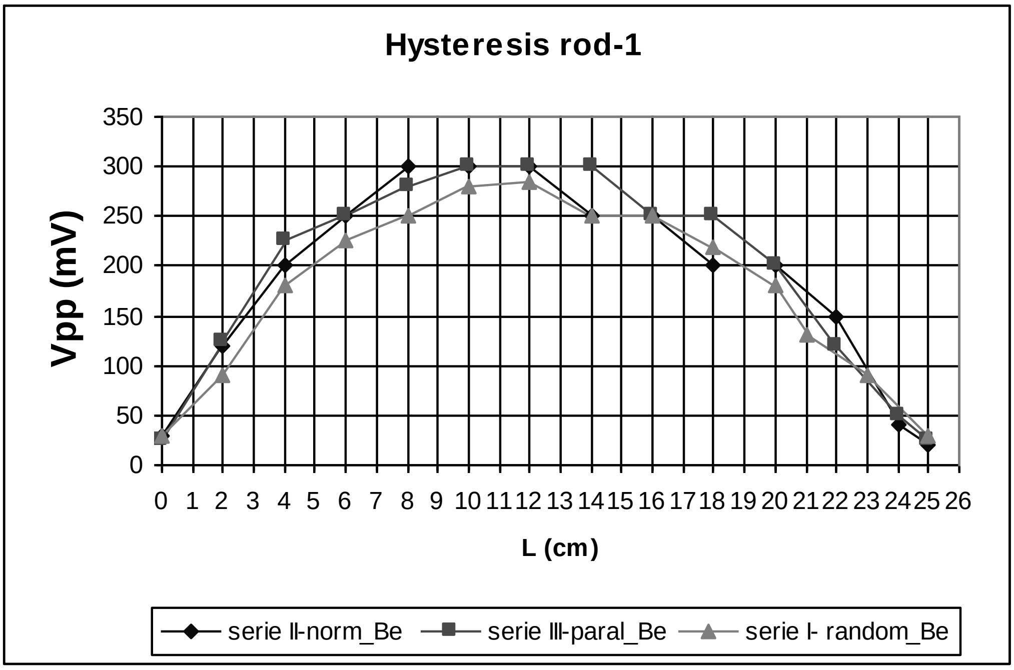

Fig.15. Results for rod-1 for $V_{coil} = 1$ V. Diagram shows three sets of measurements with different positions of the facility with respect to Earth magnetic field direction

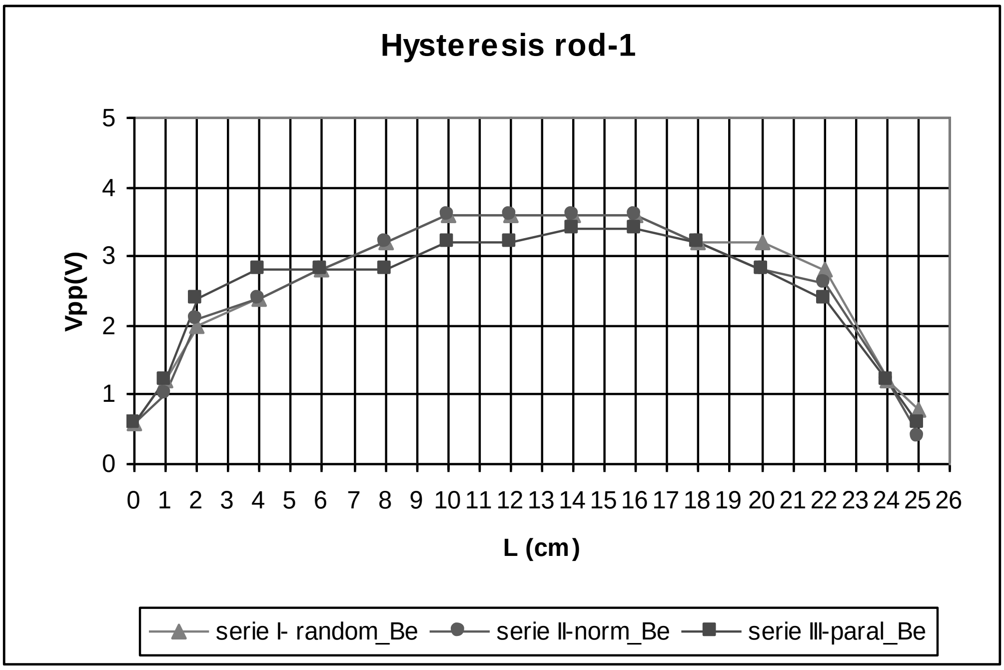

Fig.16. Results for rod-1 for $V_{coil} = 18.3$ V. Diagram shows three sets of measurements with different positions of the facility with respect to Earth magnetic field direction

7. PRELIMINARY ANALYSIS OF THE SIGNALS

A number of mathematical models are available to describe the hysteresis loop of soft magnetic material. We consider a simple approximating relation to simulate magnetization curve of hysteresis [10]:

$$B_{road} = \frac{2B_s}{\pi} \arctan\left(k(H \pm H_c)\right) \tag{7.1}$$

where $H = \frac{N_1}{L_1} i_0 \sin \omega t$. Here sign "+" is used for the ascending branch (right side of the loop) and sign "–" is used for the descending portion (left side) of the loop, $k = (\tan \frac{\pi B_r}{2B_s}) / H_c$, H_c is the coercitive force, B_r is the residual induction of the rod and B_s is the saturation flux density of permeable rod. Considering this approximation on the basis of Newman-Faraday-Lenz law the following relation for induced signal in coil-2 is obtained

$$E_{ind} = -\frac{N_2 S_2 \frac{2B_s}{\pi} \frac{1}{H_c} \tan\left(\frac{B_r \pi}{2B_s}\right) \frac{N_1}{L_1} i_0 \omega \cos \omega t}{1 + \left[\frac{1}{H_c} \tan\left(\frac{B_r \pi}{2B_s}\right)\left(\frac{N_1}{L_1} i_0 \sin \omega t \pm H_c\right)^2\right]} \tag{7.2}$$

where N_1 and N_2 are the numbers of loop of coil-1 and coil-2 respectively, L_1 is the length of solenoid, S_2 is the section of coil-2, $\omega = 2\pi f = 314$ 1/s ($f = 50$ Hz) is the pulsation and i_0 is the amplitude of current which flows through the solenoid. Graphic obtained by relation (7.2) using MATLAB tools is available in Fig.17. In this relation all material parameters are known except B_r which is variable in the range $0.45B_s - 0.65B_s$ for 4-79NM permalloy [17]. Usually it can be estimated considering $\frac{B_r}{B_s} = 0.5$ for this material (it means that $B_r = 0.4$ T) or evaluated from hysteresis loop (0.59 T). Graphical representation shows that the signal shape obtained using model (7.1) gives a good approximation for the signal shape visible in the oscilloscope (while the road is in saturation) but the voltage values are very different. This result depends on parameters B_r, B_s and H_c because we used material parameters in this simulation (road parameters can be very different).

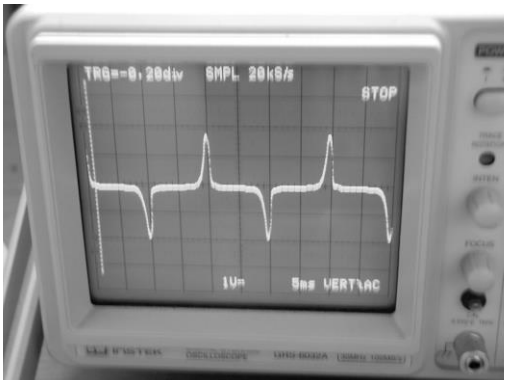

Experimental result

Analitycal result

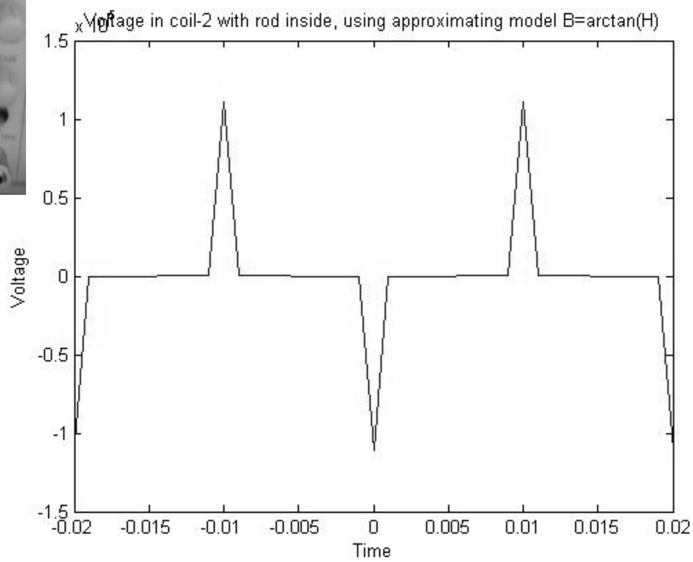

Fig.17. Mathematical results of signal in the oscilloscope obtained considering a simple approximating model (7.1) for hysteresis

If we do not put rod inside of the solenoid a mathematical relation which describes signal induced in coil 2 is more simple and it follows a cosine law

$$E_{ind} = -S_2 N_2 \frac{N_1}{L_1} \mu_0 i_0 \omega \cos \omega t \,. \qquad (7.3)$$

On the basis of this analysis we can conclude that the typical shape of signal obtained for both rods depends on hysteresis properties. To confirm these results it is necessary to repeat the tests on the others roads and to compare results.

Changing value of current in the software used to simulate this signal a signal shape changes simulating the signal shape in the oscilloscope. To try to obtain a better analytical representation of the signal obtained during the tests in laboratory when voltage $V_{coil} = 0.5$ V and $V_{coil} = 1$ V we changed empirically the function (7.2). Using two parameters (a and b) a correct approximation for the shape of this signal has been obtained. For amplitude it is necessary to multiply by a reduction factor $(1/n)$ because we used, in this preliminary simulation, material parameters. Results of this first empirical approximation while $V_{coil} = 0.5$ V are available in Fig.18. They can be compared with picture shown in Fig.11.

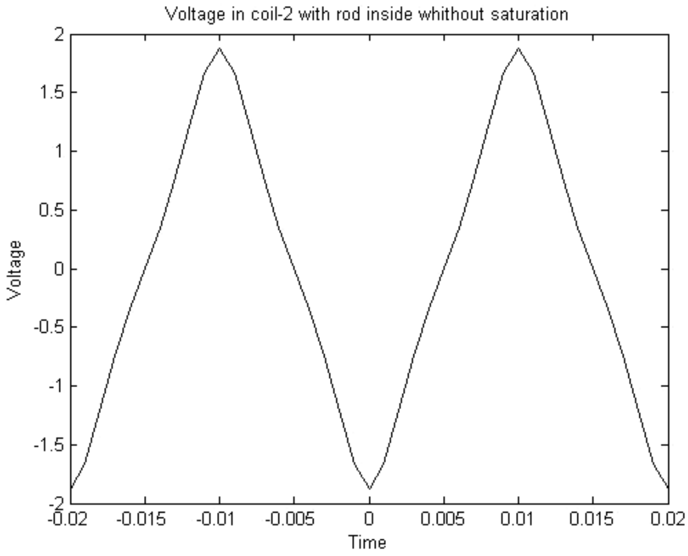

Fig.18. Analytical representation of measured signal obtained using a simple mathematical model for hysteresis loop of rod-1, $B = \arctan H$ and introducing factors a and b.

While current in the software is varied the shape of this function changes as the signal in the oscilloscope. Results for $V_{coil} = 1$ V and $V_{coil} = 2$ V are visible in Fig.19.

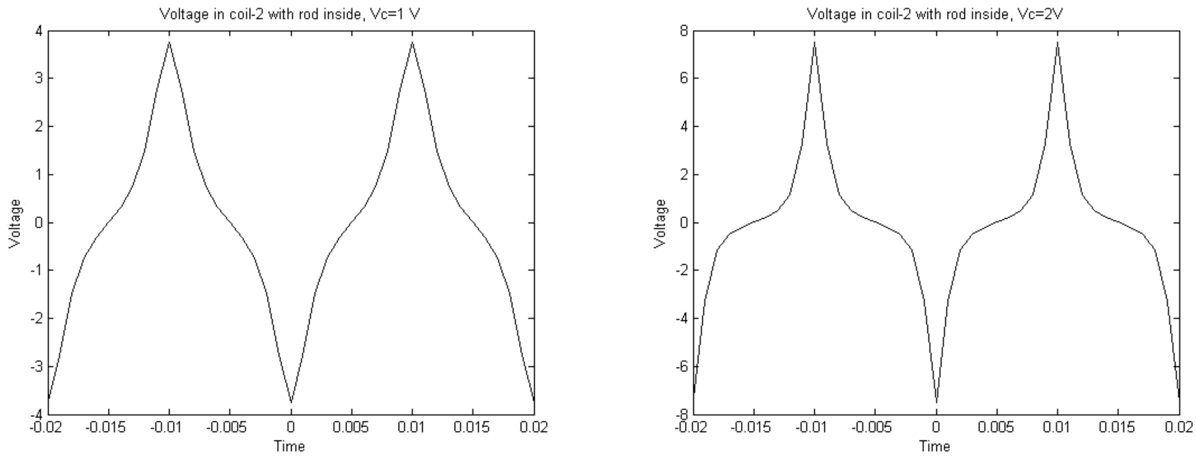

Fig.19. Analytical representation of measured signal obtained considering simple mathematical model for hysteresis loop of rod-1, $B = \arctan H$, for $V_{coil} = 1$ V (left) and $V_{coil} = 2$ V (right)

8. CONCLUSIONS AND FUTURE PLAN

Due to certain limitations we do not have the possibility to expose all experimental results obtained in the framework of this activity. In this first part we described all phases of sizing and development of a facility to carry out tests in laboratory on hysteresis rods. We described and showed tests carried out to verify correct working of this facility and after that we showed test results of the hysteresis rods. We verified experimentally that the magnetizing field in the rod is maximum in the centre of the rod length and minimum in the extremities. Changing the value of current inside of inducing coil (coil-1) we verified hysteresis rod behaviour in different configurations: normal working, approaching to the saturation and saturation. Effect of the relative position between hysteresis rod and Earth magnetic field direction has been also evaluated in all working conditions of the facility. In the last we determinate an analytical representation of signal obtained using coil-2 when hysteresis rod is arranged inside of the solenoid. This relation has been evaluated on the basis of theoretical considerations for two simple models of the hysteresis but it seems to approximate real signal shape only for values of current which correspond to $H > H_s$ of the rod. To obtain simulation of signal in normal working conditions of the rod and approaching to the saturation we modified empirically previous relations. Comparison between experimental results and pictures showed a good approximation but a more accurate analysis to interpret behaviour of signal related to rod when voltage applied to solenoid changes are requested. Tests to evaluate effects of a permanent magnet on the hysteresis rods have been also carried out. The next step of this work will be to interpret all experimental results and to try to develop a modelling for the magnetic permeability of the rod depending by its length.

9. AKNOWLEDGEMENTS

The work was supported by the Russian Foundation for Basic Research (Grants N 06-01-00389 and N 07-01-92001), the Program of the Leading Scientific Schools Support (Grant N NSh-2448.2006.1) and Italian Space Agency.

REFERENCES

[1] V.A.Sarychev and M.Yu. Ovchinnikov, *Magnetic Attitude Control Systems for Artificial Earth Satellites.* Survey of Science and Technology. Series: Exploration of Space, Moscow, 1985, VINITI, v.23, 104p.

[2] V.V.Beletskiy and A.A.Khentov, *Rotational Motion of a Magnetized Satellite.* Moscow: Nauka. Main Office of Physics and Mathematics Literature, 1985.

[3] M.Ovchinnikov, V.Pen'kov, O.Norberg and S.Barabash, *Attitude Control System for the First Swedish Nanosatellite MUNIN,* Acta Astronautica, 2000, V.46, Issue 2-6, pp.319-326.

[4] M.Yu.Ovchinnikov, V.I.Penkov, A.A.Ilyin and A.S.Selivanov, *Magnetic Attitude Control Systems for the Nanosatellite Series,* Extended Abstracts for 5th International Symposium of IAA "Small Satellites for Earth Observation", 4-8 April, 2005, Berlin, Germany, Paper IAA-B5-1201,pp.429-432

[5] F.Graziani, F.Santoni, F.Piergentili, F.Bulgarelli, M.Sgubini, M.Ronzitti, M.L.Battagliere, *UNISAT microsatellites: an affordable way to test in orbit*

innovative technologies and ideas, 23rd AIAA International Communications Satellite Systems Conference, (ICSSC-2005), 25-28 Settembre, Roma

[6] M.Yu.Ovchinnikov, A.A.Ilyin, N.V.Kupriyanova, V.I.Penkov, *Attitude dynamics of the first Russian nanosatellite TNS-0*, Acta Astronauctica, 2007, Vol.61, Issue 1-6, 277-285

[7] F.Graziani, M.Ferrante, G.B.Palmerini, F.Santoni, P.Tortora, *UNISAT Program, a University Tool for Space Education*, paper IAF-00-P.2.07, 51st International Astronautical Congress, 2-6 Oct 2000, Rio de Janeiro, Brasil

[8] F.Santoni, M.Zelli, *Passive Magnetic Attitute Stabilization of the Unisat-4 microsatellite*, 57th International Astronautical Congress, Valencia, Spain, 2-6th October 2006

[9] Ovchinnikov M.Yu., *Methods to Obtain the Principal Parameters of Simple ACS for Small Satellites*, Acta Astronautica, March 1998, V.43, Issue 11-12, pp.597-605

[10] M.Yu.Ovchinnikov and V.I.Penkov, *Passive Magnetic Attitude Control System for the Munin Nanosatellite*, Cosmic Research, Vol.40, No. 2, 2002, pp 142-156

[11] A.P.Kovalenko, *Magnetic Attitude Control Systems of Space Vehicles*, M., Mechanical Engineering, 1975, 248 p

[12] http://www.cubesatkit.com/

[13] M.Swartwout, *University-Class Satellites: from marginal utility to "Disruptive" Research Platforms*, SSC04-II-5, 18th Annual AIAA/USU, Conference on Small Satellites, Logan, UT, 9-12 August 2004

[14] M.Swartwout, *Twenty (plus) year of University-Class Spacecraft: a review of what was, an understanding of what is and look at what should be next*, 20th Annual AIAA/USU, August 2006

[15] V.A.Sarychev, V.I.Pen'kov, M.Yu.Ovchinnikov, *Mathematical Model of a Hysteresis, Based on Magnet-Mechanical Analogy*, J. Matematicheskoe Modelirovanie, 1989, v.1, N 4, pp.122-133

[16] D.Sette, M.Bertolotti, *Lezioni di Fisica 2: Elettromagnetismo e ottica*, Masson 1998, Milano, printed in Italy

[17] R.M.Bozort, *Ferromagnetism*, Van Nostrand Comapany, Reinhold, New York 1951

APPENDIX 1: LISSAJOUS'S FIGURES

Let us regard two simple harmonic motions and, at first, we consider that they have the same frequency. We can chose origin of coordinate system to have initial phase equal to zero along X axis; equation for x coordinate is

$$x = A\cos\omega t\,. \qquad \text{(A.1.1)}$$

Equation for y coordinate is

$$y = B\cos(\omega t + \delta)\,, \qquad \text{(A.1.2)}$$

where δ is the difference of phase between oscillations x and y, ω is the frequency of signals and A and B are the amplitudes; we assume $A \neq B$. Trajectory of particle is limited by line of equation $x = A$ and $y = B$. When $\delta = 0°$ two motions are in phase and equation of trajectory is

$$y = \frac{A}{B}x\,. \qquad \text{(A.1.3)}$$

This equation is represents by PQ in Fig.A.

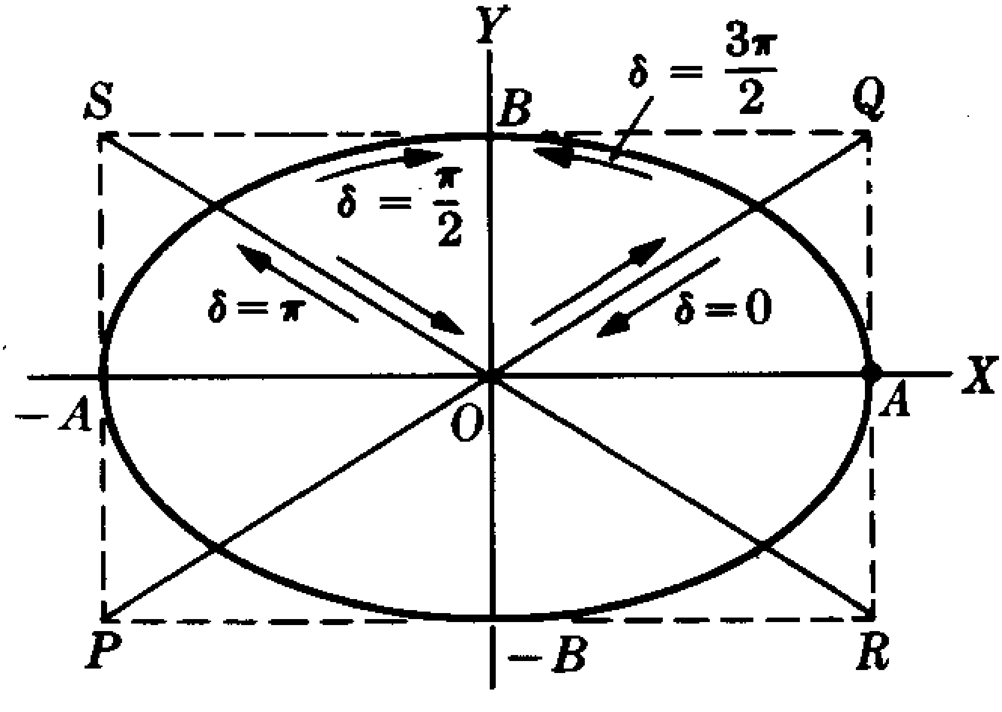

Fig.A. Composition of simple harmonic motions with the same frequency and perpendicular directions. Trajectory depends by difference of phase of two signals

If $\delta = 180°$ then $y = -B\cos\omega t$ and equation of trajectory is

$$y = -\frac{A}{B}x\,. \qquad \text{(A.1.4)}$$

This is equation is represented by RS in Fig.A. It means that for $\delta = 0°$ and $\delta = 180°$ we have a linear polarization. If $\delta = 90°$ then $y = B\cos(\omega t + \pi/2) = -B\sin\omega t$, trajectory of particle is an ellipse with equation

$$\frac{x^2}{A^2} + \frac{y^2}{B^2} = 1. \tag{A.1.5}$$

Particle moves along this ellipse in clockwise direction. To check this characteristic we evaluate velocity of particle in the point A

$$v_y = \frac{dy}{dt} = -\omega B\cos\omega t = -\omega y, \tag{A.1.6}$$

when $\delta = 270°$ (or $\delta = -90°$) trajectory of particle is again an ellipse with axis parallel to coordinate axes but particle moves along this in anticlockwise direction. It means that for $\delta = 90°$ and $\delta = -90°$ there is an elliptical polarization in the composition of two simple harmonic motions. If $A = B$ trajectory becomes a circle and we say that there is a circular polarization for the composition of two signals. For a generic value of $\Delta\delta$ trajectory is again an ellipse but with axes inclined with respect to the coordinate axes. Changing coordinate system one can demonstrate the relation between inclination of main axes of ellipse with respect to coordinate axes x and $\Delta\delta$ difference of phase of the two signal is

$$\tan\alpha = \frac{2AB\cos\Delta\delta}{A^2 - B^2}. \tag{A.1.7}$$

Some possible trajectories for different $\Delta\delta$ (difference of phase) are available in Fig.B. These trajectories are called Lissajous's Figures.

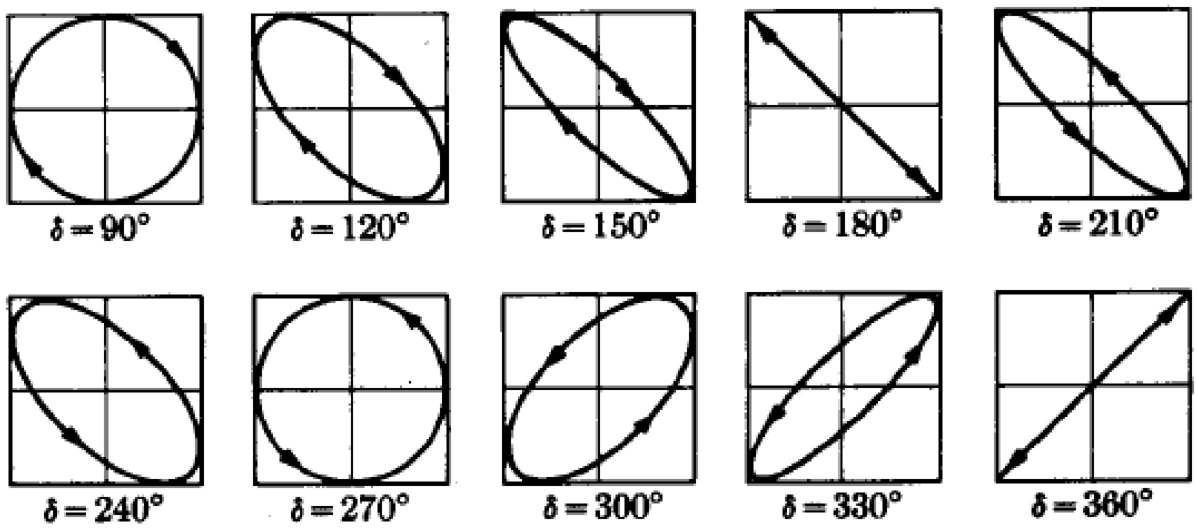

Fig.B. Possible trajectories for different Δδ between two perpendicular harmonic signals with the same frequency

Trajectory is an enclosed curve while two signals have the same frequencies. If $\omega_1 \neq \omega_2$ then the trajectory is an open curve and shape of trajectory depends on the ratio ω_2 / ω_1 and difference of phase $\Delta\delta$. Lissajous's figures for different ratio ω_2 / ω_1 and $\Delta\delta$ are sketched in Fig.C.

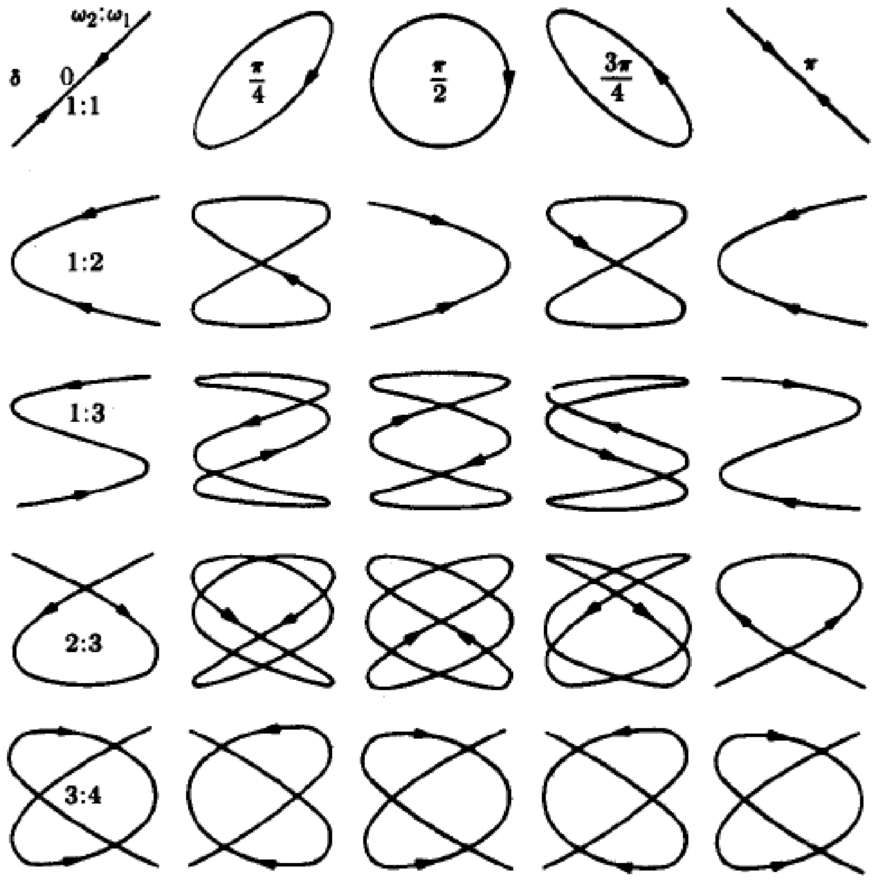

Fig.C. Trajectories for different $\Delta\delta$ between two harmonic perpendicular signals with different ratio ω_2 / ω_1

APPENDIX 2: RLC CIRCUIT

Let us consider an RLC circuit supplied by an alternative voltage $F = F_0 \sin \omega t$. Circuit equation is [16]

$$F = L\frac{di}{dt} + \frac{q}{C} + Ri. \qquad \text{(A.2.1)}$$

This is a linear differential equation similar to the equation of forced oscillations in a mechanical system. Its solution is the sum of a homogenous solution of the associate equation and of a particular integral. Homogenous solution describes transitory. We are interested in the regime solution described by particular integral. Particular solution is a current i

$$i = i_0 \sin(\omega t - \varphi)\,, \tag{A.2.2}$$

where φ is the difference of phase and $\omega = 2\pi\varphi$ ($f = 50$ Hz). To calculate i_0 and φ it needs to consider the impedance Z of circuit. Then the value of current is

$$i_0 = \frac{F_0}{Z} = \frac{F_0}{\sqrt{R^2 + (X_L + X_C)^2}}\,, \tag{A.2.3}$$

where R is the resistance, X_L is the inductive reactance ($X_L = \omega L$, where L is the inductance) and X_C is the capacitive reactance ($X_C = -\dfrac{1}{\omega C}$, where C is the capacity). To calculate the phase the following relation is used

$$\tan\varphi = \frac{X_L + X_C}{R}\,. \tag{A.2.4}$$

Voltages for R, L and C are

1) $V_R(t) = Ri(t)$
2) $V_C(t) = X_C i(t)$
3) $V_L(t) = X_L i(t)$

APPENDIX 3: LIST OF SYMBOLS

V	voltage
V_p	voltage peak (maximum amplitude)
V_{pp}	voltage peak to peak
i	current
m	magnetic dipole intensity
N_1	number of loops of coil-1
N_2	number of loops of coil-1
S_w	cross section of wire
D_w	diameter of wire
D_1	diameter of cross section of coil-1
D_2	diameter of cross section of coil-2
L_1	length of coil-1
L_2	length of coil-2
l_{w-1}	length of wire for coil 1
l_{w-2}	length of wire for coil 2
ρ	resistivity of wire
S_1	cross section of coil-1
S_2	cross section of coil-2
R_p	resistance of potentiometer
R_1	resistance of coil-1
R_2	resistance of coil-2
B	magnetic field induction
H	magnetic field intensity
H_E	Earth magnetic field intensity
Φ	magnetic flux
E_{ind}	induced electromotive force
μ_0	magnetic permeability of vacuum
X_C	capacitive reactance
X_L	inductive reactance